Ninth International Conference on
THIN-WALLED STRUCTURES – ICTWS2023
Sydney, Australia, Nov 29 – Dec 1, 2023

TESTING AND ANALYSIS OF COMPOSITE COLD-FORMED STEEL AND TIMBER FLOORING SYSTEMS WITH INNOVATIVE SHEAR CONNECTORS

Leroy Gardner*, Nathan Vella*, Spiridione Buhagiar and Pinelopi Kyvelou***

* Department of Civil and Environmental Engineering, Imperial College London, UK
e-mails: leroy.gardner@imperial.ac.uk, n.vella16@imperial.ac.uk, pinelopi.kyvelou@imperial.ac.uk

** Department of Civil and Structural Engineering, University of Malta, Malta
e-mail: spiridione.buhagiar@um.edu.mt

Keywords: Composite Beam Tests; Cold-Formed Steel; Effective Flexural Stiffness; Innovative Shear Connectors; Testing; Timber Particle Board.

Abstract. *An experimental investigation into the structural response of cold-formed steel-timber composite flooring systems with innovative and irregularly spaced shear connectors is presented in this paper. Five composite beam tests and a series of supporting material and push-out tests were carried out. The obtained results showed that the innovative shear connectors enabled the generation of considerable composite action, resulting in up to about 45% increases in load-carrying capacity and 15% and 20% increases in the initial and mid-range stiffnesses respectively over the non-composite system. Methods for predicting the effective flexural stiffness and moment capacity of the examined cold-formed steel-timber composite beams are presented and validated against the derived physical test data. It is shown that accurate predictions for both the flexural stiffness and moment capacity can be obtained, with mean prediction-to-test ratios of 1.02 and 0.94 respectively*.

1 INTRODUCTION

Flooring systems composed of cold-formed steel (CFS) beams supporting timber boards are widely used in construction, particularly in industrial and commercial applications. Retrofitting of mezzanine floor plates and the replacement of damaged slabs are examples of typical situations where use of these flooring systems is preferred, due to their dry construction method, ease of installation, high strength-to-weight ratio and the possibility for demountability and reuse [1-4]. Lightweight floor plates can, however, be prone to excessive deflections and vibrations due to their low flexural stiffness, while CFS beams are susceptible to local and distortional instabilities due to the slender nature of the cross-sections, limiting their ultimate load-carrying capacity [3,5]. Recent studies [5-9] have shown that these drawbacks can be mitigated by harnessing the composite action that can potentially develop between the timber boards and the CFS beams. Composite action shifts the position of the neutral axis such that a smaller proportion of the CFS section is in compression [7,9], while the connectors linking the two components provide partial restraint to the CFS compression flange, thus delaying the development of local and distortional instabilities [10]. In addition, increases in the flexural stiffness of the system result in reduced vibrations and deflections. The shift of the neutral axis and the increase in flexural stiffness are dependent on the degree of composite action, which is in turn dependent on the strength and slip modulus of the employed connection [6,11].

Current practice is for timber boards to be connected to the underlying CFS beams via self-drilling screws. The advantage of using such screws is mainly the fast installation process, with the screws being drilled from the top of the floorboard into the steel, eliminating the need for access from the underside while ensuring an intrinsically safe working environment. Initial

studies on CFS-timber flooring systems have therefore mainly focussed on self-drilling screws used as connectors [5-7,11], examining how their spacing influences the structural behaviour of the system.

Seeking to enhance the shear connection and, hence, the composite action in CFS-timber flooring systems, the authors initially investigated the impact of adopting inclined screws [12]. The study showed that, although there are significant benefits derived from the inclined screw configuration, these can be offset by the level of difficulty encountered when installing the screws on-site. This led the authors to develop innovative shear connectors that can be easily installed on-site and can enhance the strength and slip modulus of the connection [13,14]. The aim of the present study is to experimentally investigate the behaviour of the best performing innovative shear connectors developed in [14] when installed on a CFS-timber flooring system in bending. The study also assesses analytical solutions which may be used to predict the ultimate strength and effective flexural stiffness of the composite system.

2 MATERIAL AND SHEAR CONNECTOR TESTS

The shear connection is key to the efficiency of a composite system; therefore, previous research [12,14,15] was aimed at investigating and developing an understanding of the complex interactions at the shear interface. An overview of the conducted tests is given in this section.

2.1 Material tests

In [12], a series of material tests were carried out to determine the mechanical properties of the constituent components of the CFS-timber flooring system, namely the CFS beams, the timber boards and the connectors. The compressive properties of the wood-based particle boards were determined in accordance with BS EN 789:2004 [16], while the mechanical properties of the CFS beams were determined by means of tensile coupon tests, conducted in line with BS EN ISO 6892-1:2016 [17]. Finally, tensile tests according to BS EN ISO 898-1 [18] and BS EN ISO 6892-1:2016 [17], and bending tests according to ASTM F1575-17 [19] were carried out on the connectors of the examined floors (i.e. ordinary self-drilling screws of 5.5 mm diameter). A summary of the obtained results from all tests is presented in Table 1.

Table 1: Summary of results of material tests [12]

Component	Parameter	Average value
Particle board	Density	646 kg/m^3
	Young's modulus in compression	2.1 GPa
	Compressive strength	12.9 MPa
Cold-formed steel (1.5 mm)	Young's modulus	211 GPa
	Yield strength - 0.2% proof stress	476 MPa
	Tensile strength	566 MPa
Self-drilling screws	Young's modulus	215 GPa
	Yield strength - 0.2% proof stress	1250 MPa
	Tensile strength	1427 MPa
	Ultimate moment capacity	17,427 Nmm
	Maximum rotation (at fracture)	29.1°

2.2 Push-out tests

The shear response of several types of connectors that could be employed in the examined flooring systems, featuring screws at various orientations (i.e. perpendicular or diagonally to the board) [12] and innovative connectors [14], was examined through push-out tests, carried out according to BS EN 26891 [20].

The obtained results have shown that significant benefits in terms of stiffness can be gained when adopting inclined screws, with an increase in the slip modulus k_s [20] of up to 90% and 140% for the winged and non-winged screws respectively, and an increase in the mid-range slip modulus $k_{s,m}$ (measured between 40% and 70% of the estimated ultimate load) of up to 200% and 410% for the winged and non-winged screws respectively [12]. Despite the achieved improvements in the slip modulus, it became evident during the preparation of the test specimens that the process of driving-in inclined screws was burdensome, with the screw tip prone to break during installation. Therefore, from a practical point of view, installation of inclined screws could overcomplicate and delay construction.

Tests on innovative connectors, bespoke to the flooring systems being investigated, have shown that significant improvements in strength and slip modulus can be achieved with connectors installed perpendicularly to the shear plane, if the formation of a plastic hinge within the connector is prevented and the embedment interaction is enhanced. Six connector types were investigated in [14]. Results have shown that Type 3 and Type 4 connectors, which include a self-locking mechanism, as shown in Figure 2, achieved significant improvements in slip moduli, with increases of up to 300% and 600% for k_s and $k_{s,m}$ respectively, when compared to the equivalent values achieved by ordinary self-drilling screws installed perpendicularly to the shear plane. Improvements in the ultimate load capacity were also achieved, with increases of up to 110% when compared to ordinary screws. From a practical perspective, specimen preparation has shown that these two types of connectors are relatively easy to install and, due to their integrated self-locking mechanism, no access is required from underneath the timber board. Note that Type 3 connectors can also be fully reused if the deformations experienced during the service life of the floor plate are within typical serviceability limits.

(a) (b)

Figure 2: Dismantled and assembled connectors: (a) Type 3 and (b) Type 4 [14]

Following an assessment of all push-out tests carried out in [12] and [14], and considering both practicality of installation and performance, it was decided that two types of innovative connectors merit further investigation, Types 3 and 4; these were therefore employed in the composite beam tests described in Section 3.

3 COMPOSITE BEAM TESTS

3.1 Test specimens

Four-point bending tests were carried out to assess the flexural stiffness and moment capacity of the CFS-timber flooring system, featuring different shear connectors in various configurations, installed perpendicularly to the shear plane. Five composite beam specimens were tested in total, all comprising 1.2 m wide by 38 mm thick wood-based floorboards and two 300 mm deep and 1.5 mm thick CFS beams, spaced 600 mm apart – see Figure 3.

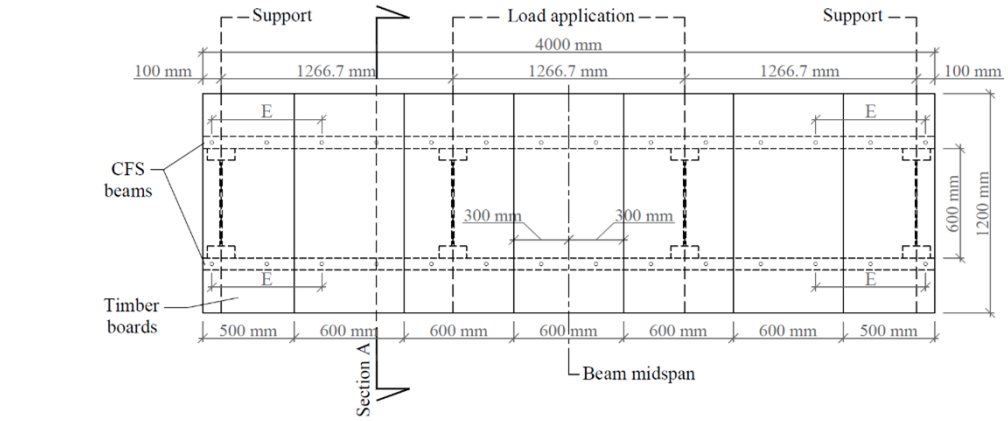

(a) Plan view

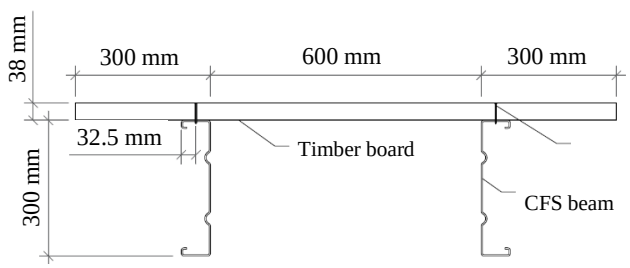

(b) Section A

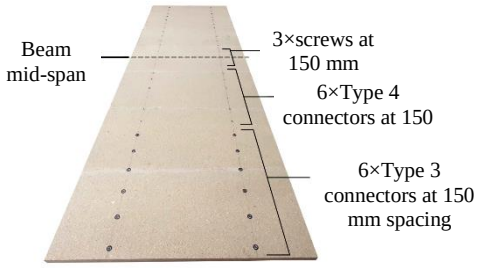

(c) Connector configuration (Specimen 5)

Figure 3: Composite beam specimen details: (a) Plan view, (b) Section A, (c) connector configuration of Specimen 5

The connectors employed for Specimen 1, the benchmark test, were ordinary screws spaced at 300 mm. Specimen 2 was similar to Specimen 1, but with the last 3 screws at the end of each beam – within the length 'E' as shown in Figure 3(a) – replaced by Type 3 innovative connectors. In Specimen 3, the same length 'E' at the end of each beam contained 9 ordinary screws at 75 mm spacing. Specimen 4 included ordinary screws spaced at 75 mm throughout the length of the beam and wood adhesive along the joints of adjacent boards to ensure their immediate contact, minimising the effect of any gaps between them. Finally, Specimen 5 comprised a combination of ordinary screws, and Type 3 and Type 4 innovative connectors, spaced at 150 mm – see Figure 3(c). A summary of the test specimens is provided in Table 2.

Table 2: Summary of composite beam test specimens

Specimen	Nominal CFS beam thickness (mm)	Connector type	Connector spacing (mm)	Wood adhesive at board joints
1	1.5	OS	300	No
2	1.5	OS + Type 3 at beam ends	300	No
3	1.5	OS	300 / 75	No
4	1.5	OS	75	Yes
5	1.5	OS + Type 3 + Type 4	150	Yes

Note: OS = Ordinary screws

3.2 Experimental layout

The test setup, shown in Figure 4, consisted of 4 m long specimens resting on rollers positioned at 100 mm from the beam ends, resulting in simply supported spans L of 3.8 m. The specimens were loaded at their third points through a spreader beam which was loaded at its midspan by a 600 kN Holmatro hydraulic cylinder. The applied loads were measured by a 200 kN load cell. As shown in Figure 4, the CFS beams were stiffened at the loading points and

supports by a 150 mm length of the same beam cross-section, connected back-to-back, and by wooden blocks, while a wooden diaphragm between the two beams was employed to prevent twisting and ensure their even loading.

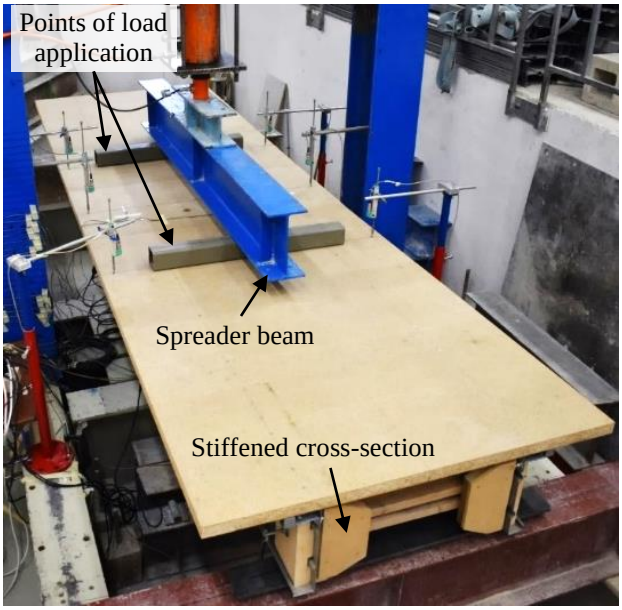

Figure 4: Composite beam test setup

Three potentiometers on each beam were employed to measure vertical displacements, at the loading points and at midspan, while four further potentiometers, one at each end of each beam, were employed to measure the interface slip between the timber boards and the CFS sections. Finally, five strain gauges were fixed on each beam section and another two at the top and bottom fibres of the timber boards at midspan, to monitor the cross-sectional strain distribution. The employed instrumentation is shown in Figure 5.

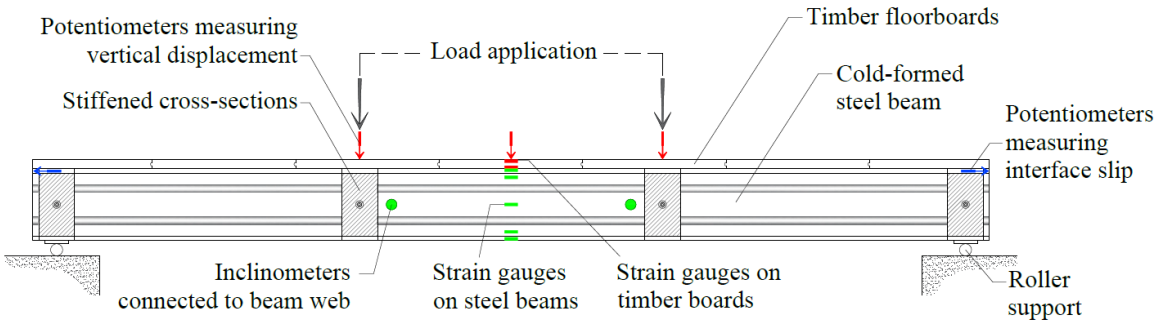

Figure 5: Instrumentation employed for composite beam tests

Four loading and unloading cycles, with a 20 kN load increase in each subsequent cycle, were applied on each specimen, followed by loading up to failure. The setup was load controlled at a rate of 2 kN/min for the loading phases and 20 kN/min for the unloading and reloading phases. All loads, displacements, strains and rotations were recorded at 0.5 s intervals, using the data acquisition software SignalExpress.

3.3 Results

The key results of the composite beam tests are presented in Table 3, where $P_{u,t}$ and $M_{u,t}$ are the maximum applied load and maximum moment per beam respectively, while $\delta_{u,t}$ and $s_{u,t}$ are the vertical displacement at midspan and the end slip at maximum load respectively. The

average values for the two beams in each test are reported. Two stiffness values were calculated for each specimen: the initial effective stiffness $(EI)_{i,t}$, calculated at a load of around $0.2P_{u,t}$ and the mid-range effective stiffness $(EI)_{mid,t}$, calculated between $0.2P_{u,t}$ and $0.6P_{u,t}$ – see Table 4.

Table 3: Composite beam test results

Specimen	$P_{u,t}$ (kN)	$M_{u,t}$ (kNm)	$\delta_{u,t}$ (mm)	$s_{u,t}$ (mm)	$(EI)_{i,t}$ (Nm^2)	$(EI)_{mid,t}$ (Nm^2)
1	46.8	29.6	31.3	1.91	1.72×10^6	1.68×10^6
2	50.3	31.8	30.8	1.03	1.83×10^6	1.80×10^6
3	50.6	32.0	30.4	1.30	1.93×10^6	1.86×10^6
4	61.4	38.8	38.9	1.86	2.07×10^6	2.00×10^6
5	67.0	42.3	48.5	1.94	1.98×10^6	1.98×10^6

The load - displacement (P_t - δ_t) curves and the load - average end slip (P_t - s_t) curves for all composite beam tests up to the ultimate load are plotted in Figure 6. Note that the unloading cycles have been removed from the curves to ensure clarity of the results. From Figure 6(a) and Table 3, it can be observed that the introduction of Type 3 fittings at the beam ends in Specimen 2 improved the ultimate load capacity and stiffness, compared to Specimen 1. Specimen 3 performed slightly better, with a higher initial stiffness and ultimate load. Specimens 4 and 5 displayed a similar load-displacement response, both performing better than all other specimens. Despite Specimen 4 being initially the stiffest, it later exhibited a reduction in stiffness with increasing load, while Specimen 5 had a stiffer response at higher loads, and reached the highest ultimate load.

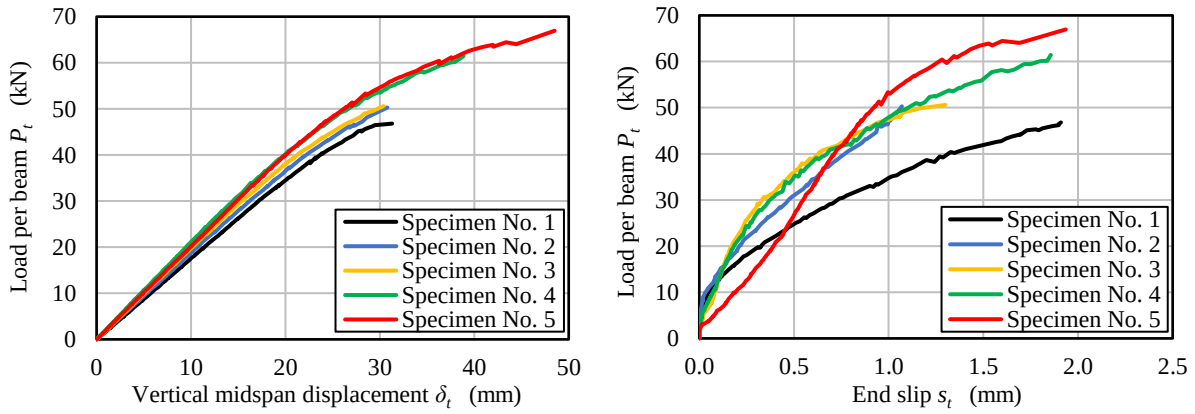

(a) (b)

Figure 6: (a) Average load-displacement curves and (b) average load-end slip curves for composite beam tests up to ultimate load

The average end slip curves shown in Figure 6(b) also indicate that Specimens 2 and 5 performed better at higher load levels. Specimen 2 displayed a steady rate of slip at higher loads, while Specimen 5 displayed a reduction in the rate of slip at mid-range loads. All other specimens experienced an increase in the rate of slip, hence a decrease in stiffness, as the loads increased. It should be noted that although Specimens 3 and 4 displayed an almost identical load-average end slip response, a proportion of slip in the third specimen would have been dissipated at each board joint until the gaps are closed and boards are in full contact; hence, this proportion of the slip was not captured by the potentiometers. Gaps at the board joints were eliminated in the final two specimens by the addition of glue. Therefore, whereas the end slip in Specimens 4 and 5 is reflective of the total interface slip resulting from midspan to the beam ends, that measured for the other three specimens that had no glue at the joints, would need to be increased by the summation of gaps between the boards.

The strain distributions at $0.5P_{u,t}$ and $P_{u,t}$, measured by the strain gauges fixed to the CFS beam and timber boards at midspan, are shown in Figure 7. It can be seen that the neutral axis shifts upwards with increasing load. This is attributed to the closure of gaps between the boards, increasing their effectiveness in transferring compressive stresses. The significant shift that occurred in Specimen 5 is also attributed to the increased effectiveness of the innovative connectors at higher slips, leading to an enhanced degree of shear connection – see Section 4.2.

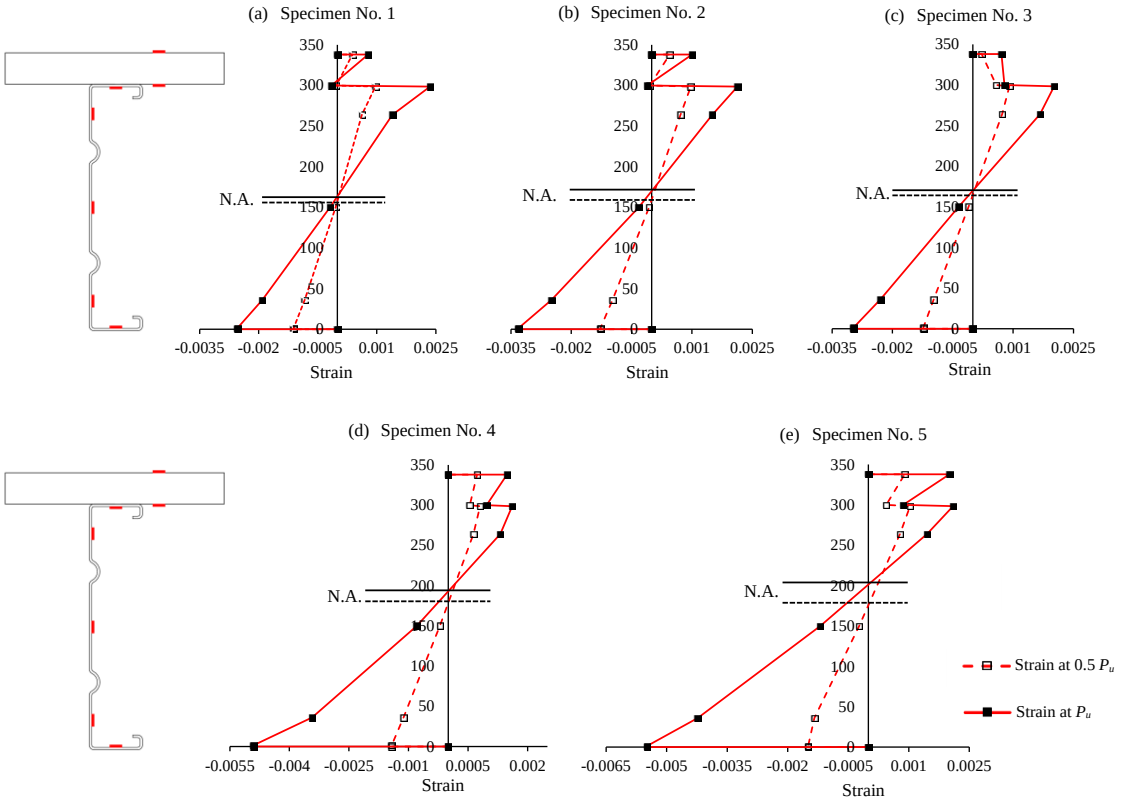

Figure 7: Strain distributions at midspan

4 ANALYSIS OF RESULTS

4.1 Flexural stiffness of CFS-timber composite beams

The flexural stiffness of composite beams is directly related to the stiffness of the shear connection at the interface between the system components. If the components are not connected and thus slip relative to each other, they act independently, with their individual cross-sectional properties, including their individual flexural stiffness, activated when subjected to bending moments. On the other hand, if the relative slip at the interface is fully restrained, the two components have full interaction and act monolithically.

A method introduced in EN 1995-1-1 [21] for determining the effective flexural stiffness of mechanically jointed timber beams, which has been recently adapted to timber-CFS composite systems [5,9], has been adopted herein for the determination of the stiffness of the examined systems. According to [5], the effective flexural stiffness $(EI)_{eff}$ of a simply supported composite beam of span L is given by Equation (1), where A_s, I_s, E_s and h are the area, second moment of area, Young's modulus and depth of the CFS section respectively, A_t, I_t, E_t and t are the area, second moment of area, Young's modulus and thickness of the overlying timber board respectively, α is the distance between the neutral axes of the CFS section and the timber board, taken as $\alpha = (t+h)/2$, γ is the shear bond coefficient given by Equation (2) and $k = K/s$ is the

smeared slip modulus at the interface, where s and K are the spacing and slip modulus of the employed connectors.

$$(EI)_{eff} = E_t I_t + E_s I_s + \frac{E_t A_t \gamma \alpha^2}{1 + \gamma \frac{E_t A_t}{E_s A_s}} \tag{1}$$

$$\gamma = \frac{1}{1 + \frac{\pi^2}{L^2} \frac{E_t A_t}{k}} \tag{2}$$

Slip measurements in [5] showed that within the critical lengths, approximately the same amount of slip is experienced by each connector, especially when these are closely spaced (i.e. $s \leq 160$ mm). Thus, when different groups of connectors are employed within the critical lengths of a beam with varying slip moduli, their average slip modulus K_{avg} can be used in place of K.

$$K_{avg} = \frac{\sum K_i n_i}{\sum n_i} \tag{3}$$

In Equation (3), K_i is the slip modulus of a connector from group i and n_i is the number of connectors in group i, with each group comprising connectors with the same slip modulus. If, on the other hand, the spacing of the connectors varies, then the average smeared slip modulus k_{avg}, given by Equation (4), should be used in Equation (2) in place of k. In Equation (4), n is the quantity of connectors within the critical length L. Note that if both the spacing and the slip moduli of the connectors are varying, the average slip modulus is first found using Equation (3) and the resulting value is then used in Equation (4) to find the average smeared slip modulus.

$$k_{avg} = \frac{Kn}{L} \tag{4}$$

Table 4 presents comparisons between the values of the effective flexural stiffness $(EI)_{eff}$ determined using the method described above and those obtained from the beam tests $(EI)_{i,t}$. Additional experimental flexural stiffness data reported in the literature [7] for simply supported composite beams with 250 mm deep CFS beams, similar to those tested herein, have also been included in the presented comparisons. It can be observed that the proposed method can accurately predict the effective flexural stiffness of the examined composite systems, with an average $(EI)_{eff}$ / $(EI)_{i,t}$ ratio of 1.02 and an associated coefficient of variation of 0.07. The validity of the proposed extension of the method to cater for irregular connector spacing and varying slip moduli is therefore demonstrated. In Figure 8(a), the flexural stiffnesses $(EI)_{i,t}$ obtained from the beam tests, normalised against the stiffnesses of the respective bare steel beams, are plotted against the shear bond coefficients γ. It can be observed that increasing values of γ lead to increases in the flexural stiffness of the examined systems, reflecting the enhanced bond at the shear interface achieved by the employed shear connectors.

4.2 Moment capacity of CFS-timber composite beams

The beneficial influence of composite action on the moment capacity of composite beams depends on the degree of shear connection at the interface between the system components. A design method devised in [5] for the determination of the degree of shear connection and, hence, of the moment capacity of CFS-timber composite systems has been appropriately adapted and applied to the specimens examined herein.

The force to be transferred by the connectors in a system with full shear connection V is limited either by the compressive strength of the timber boards $F_{c,t}$ or by the tensile strength of the CFS section $F_{t,s}$. Note that for the systems examined herein, consisting of beams spaced at 600 mm, physical tests [7] and numerical simulations [11] have shown that there is no evidence of shear lag across the width of the board. The number of shear connectors required per critical length, as defined in [22], for a fully composite system n_f can be determined from Equation (5), where F_v is the shear force that can be withstood by each connector and may either be determined from push-out test data or using the methodology presented in [14,15].

$$n_f = \frac{n}{F_v} \tag{5}$$

As described in [5], the plastic moment capacity $M_{pl,comp}$ of a fully composite system can be determined based on cross-sectional equilibrium. The derived formulae depend on the position of the plastic neutral axis (PNA), which can be located within the timber board, within the CFS beam or at their interface. Note that CFS sections are typically classified as Class 3 or Class 4 and, thus, have their moment resistance limited to either the elastic or the effective moment capacity due to local instabilities. However, for a composite system with full shear connection, the compression flange of the CFS section is restrained by the overlying board, while a reduced extent of the CFS web is under compression due to the upward shift of the neutral axis. When the total strength of the shear connectors provided within a critical length is less than that required to develop full shear connection, the shear connection is partial. The degree of shear connection η_d, for a system consisting of n connectors of the same properties is given by Equation (6). If the connectors are not the same, then Equation (7) can be used instead, where $F_{v,i}$ is the shear strength of the i^{th} connector.

$$\eta_d = \frac{n}{n_f} \leq 1 \tag{6}$$

$$\eta_d = \frac{\sum F_{v,i}}{V} \leq 1 \tag{7}$$

In Figure 8(b), the moment capacities $M_{u,t}$ obtained from the beam tests performed herein and in [7], normalised by the moment capacities of the respective bare steel sections, are plotted against the degree of composite action η_d. As expected, increasing values of η_d led to increases in the capacity of the examined systems, reflecting the composite action mobilised by the shear connectors.

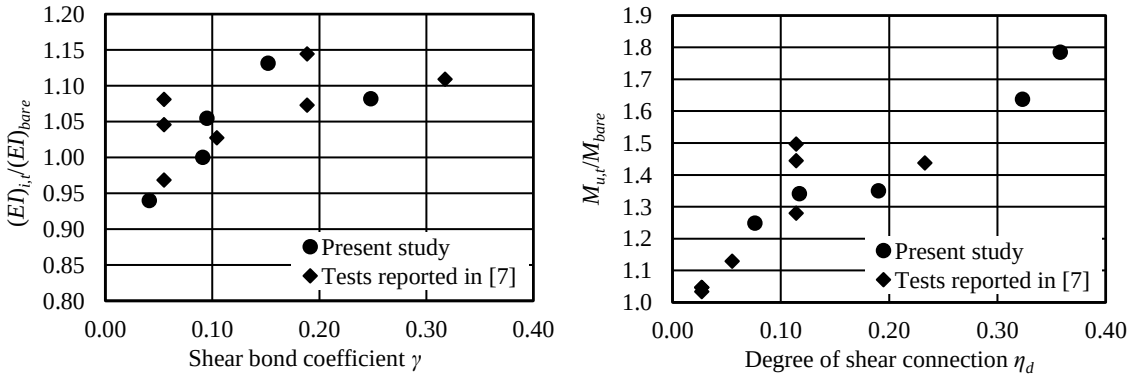

Figure 8: Increases in (a) flexural stiffness and (b) moment capacity of composite specimens relative to bare steel sections

An extension of the EN 1994-1-1 [22] design approach for determining the moment capacity of composite steel-concrete systems comprising Class 1 or 2 steel sections with partial shear connection to CFS-timber systems with Class 3 or 4 sections was introduced in [5]. As shown in Figure 9, this approach [5] can be used to determine the moment capacity of a CFS-timber composite system either based either on plastic theory using Equation (8), or on a more conservative simplified linear expression, as given by Equation (9).

$$M_{c,Rd} = M_{pl,Rd} - (1-\eta_d)\,(M_{pl,bare} - M_{bare}) \tag{8}$$

$$M_{c,lin,Rd} = M_{bare} + \eta_d\,(M_{pl,comp} - M_{bare}) \tag{9}$$

In Equations (8) and (9), $M_{pl,Rd}$ and $M_{pl,bare}$ are the plastic moment capacities of the composite system with partial shear connection and the bare steel section respectively, $M_{pl,comp}$ is the plastic moment capacity of the fully composite system, while M_{bare} is the elastic or the effective moment capacity (depending on the classification of the cross-section) of the bare steel section [23]. Note that, in line with the recommendations set out in [5], when $\eta_d < 0.05$, no composite action should be considered, and the moment capacity of the system should be limited to that of the bare steel section M_{bare}.

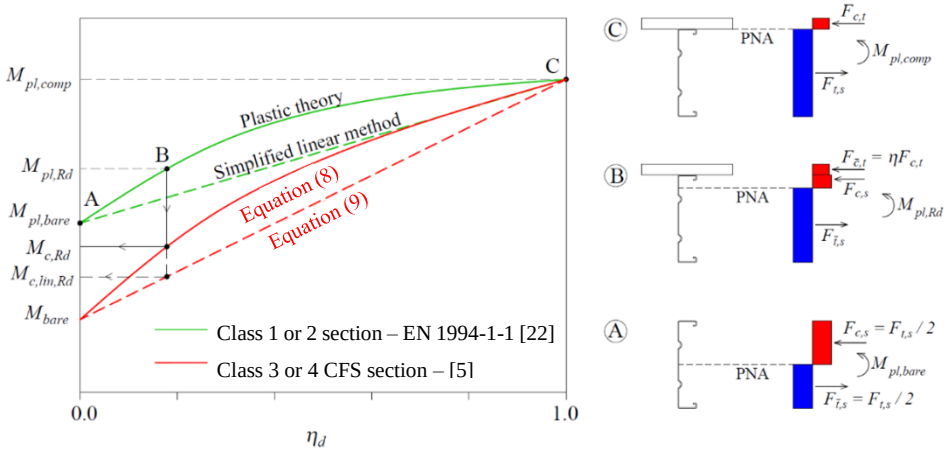

Figure 9: Variation of moment capacity with degree of shear connection for a composite system with a Class 1 or 2 steel section – EN 1994-1-1 [22] and a Class 3 or 4 CFS section [5]

Comparisons between the moment capacities predicted by the method described above and the experimental results $M_{u,t}$ are presented in Table 4, where the experimental data reported in [7] have also been included. It can be observed that the adopted design approach yields accurate results, while the comparisons confirm that the approach based on the plastic theory is more accurate than the simplified linear expression, with average prediction-to-test ratios equal to 0.94 and 0.88 respectively, and a coefficient of variation equal to 0.07 for both methods.

Table 4: Comparisons between effective flexural stiffness and moment capacity predicted by proposed method and obtained from the test results

Specimen	$(EI)_{eff}$ (Nm^2)	$(EI)_{i,t}$ (Nm^2)	$(EI)_{eff}$ / $(EI)_{i,t}$	$M_{c,Rd}$ (kNm)	$M_{c,lin,Rd}$ (kNm)	$M_{u,t}$ (kNm)	$M_{c,Rd}$ / $M_{u,t}$	$M_{c,lin,Rd}$ / $M_{u,t}$
1	1.89×10^6	1.72×10^6	1.10	28.1	26.3	29.6	0.95	0.89
2	1.96×10^6	1.83×10^6	1.07	30.4	27.7	31.8	0.96	0.87
3	1.96×10^6	1.93×10^6	1.02	34.1	30.2	32.0	1.07	0.94
4	2.04×10^6	2.07×10^6	0.98	40.2	34.7	38.8	1.04	0.89
5	2.15×10^6	1.98×10^6	1.09	41.6	35.9	42.3	0.98	0.85
B15-2*	1.18×10^6	1.20×10^6	0.99	19.1**	19.1**	20.0	0.95	0.95
B15-3*	1.31×10^6	1.27×10^6	1.03	24.5	22.0	27.6	0.89	0.80

B15-4*	1.31×10^6	1.57×10^6	0.83	24.5	22.0	28.6	0.86	0.77
B30-2*	2.25×10^6	2.13×10^6	1.05	46.4**	46.4**	48.6	0.96	0.96
B30-3*	2.25×10^6	2.30×10^6	0.98	46.4**	46.4**	48.0	0.97	0.97
B30-4*	2.30×10^6	2.26×10^6	1.02	49.0	48.2	52.4	0.94	0.92
B30-5*	2.38×10^6	2.36×10^6	1.01	51.7	50.2	59.4	0.87	0.85
B30-6*	2.51×10^6	2.44×10^6	1.03	56.9	54.2	66.7	0.85	0.81
		AVERAGE	**1.02**				**0.94**	**0.88**
		COV	**0.07**				**0.07**	**0.07**

* Experimental results reported in [7]

** $M_{c,Rd} = M_{bare}$ since $\eta_d < 0.05$

4.3 Performance of innovative shear connectors in composite beam systems

It is evident from Table 4 that for the specimens with the innovative shear connectors (i.e. Specimens 2 and 5), the initial stiffness determined from the experiments was lower, by 8% on average, than that predicted by the method presented in Section 4.1. The lower initial stiffnesses are attributed to the initial tolerance gaps between the different connector components. From Figure 6(b), it can be seen that there was very little slip in the initial stages of loading, generally less than 0.5 mm end slip for loads up to around 50% of the ultimate. This means that even the slightest tolerance gaps had a significant impact on the initial stiffness of the system. It is only when the generated slip is sufficient to bring all the individual components into direct contact that the connector can be deemed to be fully effective.

5 CONCLUSIONS

An experimental investigation into the structural response of CFS-timber composite flooring systems, featuring a combination of ordinary self-drilling screws and innovative shear connectors, has been presented. It has been shown that the performance of the innovative connectors improves with increasing load, with this trend being attributed to the closure of tolerance gaps between the various connector components as the interface slip increases. The best performing specimen, comprising a combination of ordinary screws and innovative connectors at 150 mm spacing, achieved increases of up to about 45% in moment capacity and almost 20% in mid-range stiffness, when compared to the benchmark specimen with ordinary screws at 300 mm spacing, while the respective increases in capacity were up to 80% compared to the bare steel section (which is currently considered in design as the sole load bearing component of the system).

The applicability of design methods reported in the literature for the calculation of the effective flexural stiffness and moment capacity of CFS-timber composite systems has been evaluated by comparisons against the obtained experimental data. In addition, these methods have been adapted to cater for varying screw spacings and varying connector strengths, and it has been shown that accurate predictions of the effective stiffness and moment capacity of the examined systems can be achieved, with mean prediction-to-test ratios of 1.02 and 0.94 respectively.

REFERENCES

[1] Kelly A. and Zweben C., *Comprehensive Composite Materials*, Elsevier, Pergamon Press, 2000.

[2] Hassanieh A., Valipour H.R. and Bradford M.A., "Experimental and analytical behaviour of steel-timber composite connections", *Construction and Building Materials*, **118**, 63-75, 2016.

[3] Cicione, A. and Walls, R., "The effect of shear connectors on the strength, serviceability and dynamic response of composite floors using cold-formed steel beams and concrete in decking", *Engineering Structures*, **269**, 114806, 2022.

[4] Navaratnam S., Widdowfield Small D., Gatheeshgar P., Poologanathan K., Thamboo J., Higgins C. and Mendis P., "Development of cross laminated timber-cold-formed steel composite beam for floor system to sustainable modular building construction", *Structures*, **32**, 681-690, 2021.

[5] Kyvelou, P., Gardner, L. and Nethercot, D.A., "Design of Composite Cold-Formed Steel Flooring Systems", *Structures*, **12**, 242-252, 2017.

[6] Kyvelou, P., Gardner, L. and Nethercot, D.A., "Composite Action Between Cold-Formed Steel Beams and Wood-Based Floorboards", *International Journal of Structural Stability and Dynamics*, **15**(8), 1540029, 2015.

[7] Kyvelou, P., Gardner, L. and Nethercot, D.A., "Testing and Analysis of Composite Cold-Formed Steel and Wood-Based Flooring Systems", *Journal of Structural Engineering*, **143**(11), 04017146, 2017.

[8] Gandomkar, F.A., Wan Badaruzzaman, W.H., Osman, S.A. and Ismail, A., "Experimental and numerical investigation of the natural frequencies of the composite profiled steel sheet dry board (PSSDB) system", *Journal of the South African Institution of Civil Engineering*, **55**, 11-21, 2013.

[9] Kyvelou, P., Reynolds, T.P.S., Beckett, T.S.C. and Huang, Y., "Experimental investigation on composite panels of cold-formed steel and timber", *Engineering Structures*, **247**, 113186, 2021.

[10] Shi, Y., Yang, K., Guan, Y., Yao, X., Xu, L. and Zhang, H., "The flexural behaviour of cold-formed steel composite beams", *Engineering Structures*, **218**, 110819, 2020.

[11] Kyvelou, P., Gardner, L. and Nethercot, D.A., "Finite Element Modelling of Composite Cold-Formed Steel Flooring Systems", *Engineering Structures*, **158**, 28-42, 2018.

[12] Vella, N., Gardner, L. and Buhagiar, S., "Experimental analysis of cold-formed steel-to-timber connections with inclined screws", *Structures*, **24**, 890-904, 2020.

[13] Kyvelou, P., Nethercot, D.A., Hadjipantelis, N., Kyprianou, C. and Gardner, L., "The evolving basis for the design of light gauge steel systems", *International Journal of Structural Stability and Dynamics*, **20**(13), 2041008, 2020.

[14] Vella, N., Kyvelou, P., Buhagiar, S. and Gardner, L., "Innovative shear connectors for composite cold-formed steel-timber structures: an experimental investigation", *Engineering Structures*, [submitted] (2023).

[15] Vella, N., Gardner, L. and Buhagiar, S., "Analytical modelling of cold-formed steel-to-timber connections with inclined screws", *Engineering Structures*, **249**, 113187, 2021.

[16] EN 789, *Timber structures – Test methods – Determination of mechanical properties of wood based panels*, European Committee for Standardisation, Brussels, 2004.

[17] EN ISO 6892-1, *Metallic materials – Tensile testing. Part 1: Method of test at room temperature*, European Committee for Standardisation, Brussels, 2016.

[18] EN ISO 898-1, *Mechanical properties of fasteners made of carbon steel and alloy steel*, European Committee for Standardisation, Brussels, 2013.

[19] ASTM Standard F1575, *Standard Test Method for Determining Bending Yield Moment of Nails*, ASTM International, West Conshohocken, PA, 2017.

[20] EN 26891, *Timber structures – Joints made with mechanical fasteners – General principles for the determination of strength and deformation characteristics*, European Committee for Standardisation, Brussels, 1991.

[21] EN 1995-1-1. *Eurocode 5: Design of timber structures. Part 1-1: General – Common rules and rules for buildings*, European Committee for Standardisation, Brussels, 2004.

[22] EN 1994-1-1. *Eurocode 4: Design of composite steel and concrete structures. Part 1-1: General rules and rules for buildings*, European Committee for Standardisation, Brussels, 2004.

[23] EN 1993-1-3. *Eurocode 3: Design of steel structures. Part 1-3: General rules – Supplementary rules for cold-formed members and sheeting*, European Committee for Standardisation, Brussels, 2006.